Clinical and Experimental Immunology, 2022, **207**, 241–252
https://doi.org/10.1093/cei/uxab030
Advance access publication 14 December 2021
Research Article

Clinical & Experimental IMMUNOLOGY

OXFORD

Research Article

LncRNA MIR155HG functions as a ceRNA of miR-223-3p to promote cell pyroptosis in human degenerative NP cells

Wei Yang, Xu-Dong Huang, Tao Zhang, You-Bin Zhou, Yong-Cheng Zou and Jian Zhang*

The First Affiliated Hospital, Orthopedic Center, Hengyang Medical School, University of South China, Hengyang, Hunan, China

*Correspondence: Jian Zhang, The First Affiliated Hospital, Orthopedic Center, Hengyang Medical School, University of South China, Hengyang, Hunan, 421001, China. Email: 462192195@qq.com

Abstract

Nucleus pulposus (NP) cell pyroptosis plays a critical role in the pathogenesis of intervertebral disk degeneration (IDD). MIR155 host gene (MIR155HG) is a long non-coding RNA with pro-inflammatory activity. However, very little is known about its role in NP cell pyroptosis. This study aimed to observe the impact of MIR155HG on cell pyroptosis and to explore the underlying mechanism in human degenerative NP cells. Our results demonstrated that MIR155HG expression was significantly increased in human degenerative NP tissue samples and showed a positive correlation with Pfirrmann score. Overexpression of MIR155HG through a lentiviral vector decreased miR-223-3p levels, up-regulated NLRP3 expression and induced cell pyroptosis in human degenerative NP cells. A ceRNA action mode was identified among MIR155HG, miR-223-3p, and NLRP3. The stimulatory effect of MIR155HG on human degenerative NP cell pyroptosis was significantly reversed by pretreatment with miR-223-3p mimic or NLRP3 siRNA. In summary, these data suggest that MIR155HG sponges miR-223-3p to promote NLRP3 expression, leading to induction of cell pyroptosis in human degenerative NP cells. Targeting MIR155HG could be a novel and promising strategy to slow down the progression of IDD.

Keywords: MIR155HG, miR-223-3p, NLRP3, pyroptosis, ceRNA, IDD

Abbreviations: ceRNAs: competing endogenous RNAs; ELISA: enzyme-linked immunosorbent assay; FBS: fetal bovine serum; IDD: intervertebral disk degeneration; IL: interleukin; lncRNAs: long non-coding RNAs; LBP: low back pain; LDH: lactate dehydrogenase; LVF: lumbar vertebral fracture; miRNAs: microRNAs; MIR155HG: MIR155 host gene; NLRP3: nucleotide-binding oligomerization domain-like receptor protein 3; NP: nucleus pulposus; GSDMD-N: Gasdermin N-terminal fragment; qRT-PCR: quantitative real-time PCR; siRNA: small interfering RNA; TNF-α: tumor necrosis factor-α.

Introduction

Low back pain (LBP) has become a major public health problem across the world with a heavy socio-economic burden [1]. As the most frequent cause of LBP, intervertebral disk degeneration (IDD) is closely associated with nucleus pulposus (NP) cell death and inflammatory response [2, 3]. Pyroptosis is a newly discovered type of programmed cell death, which is characterized by activation of nucleotide-binding oligomerization domain-like receptor protein 3 (NLRP3) inflammasome and abundant release of interleukin (IL)-1β and IL-18 [4]. Several lines of evidence have demonstrated that prevention of NP cell pyroptosis slows down the progress of IDD in animal models [5, 6]. Current treatments for IDD include conservative management and surgical intervention, but these therapeutic methods are only restricted to relieve LBP and do not target its pathophysiological processes. Therefore, a more detailed understanding of the regulatory mechanisms responsible for NP cell pyroptosis is important to develop novel therapeutic approaches for degenerative disk disease.

Long non-coding RNAs (lncRNAs) are a class of RNA transcripts with a length greater than 200 nucleotides and have no protein-coding capacity. There is accumulating evidence that dysregulation of lncRNAs plays an important role in the onset and development of IDD [7–9]. MIR155 host gene (MIR155HG), a newly discovered lncRNA, is located on chromosome 21q21 in humans. In peripheral blood mononuclear cells-derived macrophages isolated from patients with chronic obstructive pulmonary disease, MIR155HG overexpression induces the phenotypic transition from M2 to M1 and promotes the production of tumor necrosis factor-α (TNF-α), IL-1β, and IL-12 [10]. In contrast, knockdown of MIR155HG by small interfering RNA (siRNA) inhibits the release of TNF-α, IL-6, and IL-8 in human pulmonary microvascular endothelial cells exposed to cigarette smoke extract [11]. Another study showed that silencing of MIR155HG dramatically suppresses inflammatory response in RAW 264.7 cells treated with lipopolysaccharide [12]. These results suggest that MIR155HG is a pro-inflammatory lncRNA. However, it is unclear whether this lncRNA regulates cell pyroptosis and inflammation in human degenerative NP cells.

MicroRNAs (miRNAs) are a class of non-coding single-stranded RNA molecules ranging from 20 to 25 nucleotides in length and function as the post-transcriptional regulators of gene expression. We and others previously reported that aberrant expression of miRNAs is linked to

Received 17 September 2021; Revised 19 November 2021; Accepted for publication 26 November 2021

IDD progression [13–16]. The miR-223 encoding gene is located on the q12 locus of the X chromosome [17]. It has been reported that miR-223 can attenuate the persistent pain after lumbar disc herniation in rats [18]. Additionally, miR-223 inhibits inflammatory response in rat NP cells challenged with lipopolysaccharide [19]. NLRP3, a nuclear component of the NLRP3 inflammasome, senses various pathogen-associated molecular patterns (PAMPs) and danger-associated molecular patterns. As a major subtype of miR-223, miR-223-3p is known to suppress cell pyroptosis by targeting NLRP3 in multiple cell types, including endothelial cells [20], gastric cancer cells [21], and fibroblast-like synoviocytes [22]. Competing endogenous RNAs (ceRNAs) are RNA transcripts that cross-regulate each other by competing for shared miRNAs [23, 24]. Dysregulation of the ceRNA network plays an important role in the pathogenesis of IDD [25–27]. However, whether there is a ceRNA regulatory network present among MIR155HG, miR-223-3p and NLRP3 is poorly understood.

In the present study, we found that MIR155HG was highly expressed in human degenerative NP tissue and its expression levels showed a positive correlation with Pfirrmann score. Importantly, MIR155HG acted as a ceRNA of miR-223-3p to up-regulate NLRP3 expression and induce cell pyroptosis in human degenerative NP cells. This is the first time to demonstrate an association of MIR155HG with NP cell pyroptosis.

Materials and methods

Cells, reagents, and antibodies

The 293T cells were purchased from American Type Culture Collection (Rockville, MD, USA). Dulbecco's Modified Eagle Medium (DMEM)/F12 was provided by Gibco (Grand Island, NY, USA). Fetal bovine serum (FBS) and Hoechst 33342/propidium iodide (PI) double stain kit were obtained from Sigma-Aldrich (St. Louis, MO, USA) and Solarbio (Beijing, China), respectively. NLRP3 rabbit polyclonal antibody, caspase-1 rabbit polyclonal antibody, Gasdermin N-terminal fragment (GSDMD-N) rabbit monoclonal antibody, and β-actin mouse monoclonal antibody were supplied by Abcam (Cambridge, UK). Horseradish peroxidase (HRP)-conjugated goat anti-rabbit IgG (H+L) and HRP-conjugated goat anti-mouse IgG (H+L) were from Beyotime (Shanghai, China).

Clinical NP tissue samples

Normal NP tissue samples were collected from patients with lumbar vertebral fracture (LVF) without any history of low back pain (n = 10; 5 females, 5 males; mean age 21.67 years, range 18–26 years). Degenerative NP tissue samples were collected from IDD patients (n = 30; 13 females, 17 males; mean age 54.32 years, range 42–65 years). All samples were obtained by discectomy and intervertebral fusion surgery under sterile conditions and processed within 1 h of being harvested. Grading was evaluated according to the Pfirrmann classification by magnetic resonance imaging of the disc. The samples from IDD patients were grades III–V with 10 samples in each grade, and the samples from LVF patients were grade II. The experimental protocols were approved by the Ethics Committee of the First Affiliated Hospital of University of South China. The informed consent was obtained from each patient.

Isolation and culture of human degenerative NP cells

Human degenerative NP cells were isolated and cultured as previously described [28]. Briefly, 10 degenerative NP samples with grade IV were cleaved into 1 mm^3 of small fragments using an ophthalmic scissor after washing with PBS twice. These fragments were digested in 0.25% trypsin solution (Sigma-Aldrich) and then treated with 0.2% type II collagenase (Sigma-Aldrich) at 37°C for 4 h. The resulting cells were cultured in DMEM/F12 medium containing 15% FBS and 1% penicillin-streptomycin in a humidified atmosphere with 5% CO_2 at 37°C. The medium was replaced twice per week. Cells in the second generation were used for the *in vitro* experiments.

Lentivirus infection

Lentiviral vector expressing MIR155HG (LV-MIR155HG) and empty vector (LV-Mock) were obtained from Genechem (Shanghai, China). When human degenerative NP cells reached a confluence of 70-80%, cells were seeded into a 24-well plate (2×10^5 cells/well). Afterwards, cells were infected with LV-Mock or LV-MIR155HG at a multiplicity of infection of 100 in the presence of 8 mg/ml of polybrene. Cells in control group were treated with PBS. Twenty-four hours later, cells were incubated in fresh DMEM/F12 medium supplemented with 10% FBS for an additional 48 h. The expression levels of MIR155HG were measured using quantitative real-time PCR (qRT-PCR) to evaluate the transfection efficiency.

Silencing of NLRP3 by siRNA

The siRNA against NLRP3 (forward: 5′-CAACAGGAGAGACCUUUAUTT-3′, reverse: 5′-AUAAAGGUCUCUCCUGUUGTT-3′) and scrambled siRNA as a negative control were synthesized by GenePharma (Shanghai, China). Human degenerative NP cells plated in 24-well plates (2×10^5 cells/well) were transfected with the above siRNAs at a final concentration of 40 nM using Lipofectamine 3000 (Invitrogen, Carlsbad, CA, USA) according to the manufacturer's instructions. After 48 h of transfection, western blot was conducted to determine gene-silencing efficacy.

Bioinformatics prediction and luciferase reporter assay

The online softwares including TargetScan (http://www.targetscan.org/) and miRDB (http://mirdb.org/miRDB/) were used to predict the binding site between miR-223-3p and NLRP3 3′ untranslated region (UTR). The free energy score for the interaction between miR-223-3p and NLRP3 3′UTR was evaluated by the RNAhybrid database (http://bibiserv.techfak.uni-bielefeld.de/rnahybrid/submission.html). The binding site between MIR155HG and miR-223-3p was predicted by the Starbase database (http://starbase.sysu.edu.cn/). Subsequently, PCR was employed to amplify NLRP3 3′UTR and MIR155HG sequences with the putative miR-223-3p binding site from human degenerative NP cells. These amplified products were cloned into the pmirGLO dual-luciferase miRNA target expression vectors (Promega, Madison, WI, USA) to construct pmirGLO-wild type NLRP3 and MIR155HG plasmids (NLRP3-WT and MIR155HG-WT). The corresponding mutant plasmids were also produced by

mutating the miR-223-3p binding site, designated as NLRP3-Mut and MIR155HG-Mut. The 293T cells were seeded in a 24-well plate and cultured in DMEM medium containing 10% FBS and 1% penicillin-streptomycin in a humidified atmosphere with 5% CO_2 at 37°C. After reaching a confluence of 70% to 80%, cells were co-transfected with the above plasmids (1 μg) and miR-223-3p mimic/mimic control (50 nM) by using Lipofectamine 3000 (Invitrogen) for 48 h. The firefly and renilla luciferase activities were detected using a dual-luciferase reporter assay system (Promega). The firefly luciferase activity was normalized to the renilla luciferase activity.

Transfection with miR-223-3p mimic/inhibitor

The mimic and inhibitor of miR-223-3p and their respective negative controls were chemically synthesized by Ribobio (Guangzhou, China). Human degenerative NP cells at a confluence of 70% to 80% were transfected with 50 nM of miR-223-3p mimic, mimic control, miR-223-3p inhibitor or inhibitor control using Lipofectamine 3000 (Invitrogen). Forty-eight hours later, cells were harvested for further analyses.

Hoechst 33342/PI double fluorescence staining

The Hoechst 33342/PI double fluorescence staining was carried out according to a previously reported method [29]. At the end of the indicated treatment, human degenerative NP cells were harvested and then stained with 10 μl of Hoechst 33342 solution at 37°C in the dark for 10 min. Thereafter, cells were stained with 5 μl of PI at 37°C in the dark for 10 min. The stained cells were observed and photographed under a fluorescence microscope (Olympus IX53, Tokyo, Japan).

Pulldown assay with biotinylated miR-223-3p (bio- miR-223-3p)

Biotin pulldown was performed according to a previously reported method [30]. In brief, human degenerative NP cells were transfected with bio-miR-223-3p-WT, bio-miR-223-3p-Mut or bio-miRNA negative control (bio-miR-NC) using Lipofectamine 3000 (Invitrogen). After 48 h of transfection, cells were washed with PBS and then lysed on ice for 10 min. Cell lysates were collected and then incubated with M-280 streptavidin magnetic beads (Sigma-Aldrich) at 4°C for 4 h. To exclude RNA and protein complexes, the beads were blocked in lysis buffer containing RNase-free bovine serum albumin (Beyotime) and yeast tRNA (Sigma-Aldrich). The beads were washed twice with the lysis buffer, three times with low-salt buffer, and once with high-salt buffer. The TRIzol reagent (Invitrogen) was employed to isolate the bound RNAs, followed by detection of MIR155HG expression using qRT-PCR.

Detection of lactate dehydrogenase (LDH) release

LDH release was detected using the LDH assay kit (Beyotime) according to the manufacturer's instructions. In brief, the medium was centrifuged at 400 ×*g* for 5 min to collect the supernatants. Then, 25 μl cell culture supernatants and 25 μl substrates were mixed together. After 15 min of incubation at 37°C, 25 μl 2,4-dinitrophenylhydrazine was added to each sample and incubated at 37°C for 15 min. Finally, 250 μl of 0.4 mol/l NaOH solution was added and incubated at room temperature for 5 min. The absorbance at 490 nm was measured using a spectrophotometric microplate reader (PerkinElmer, Waltham, MA, USA). Background optical absorbance was detected at 690 nm and subtracted from primary measurements for each well. The LDH activity in the medium was calculated using a concurrent standard curve.

Enzyme-linked immunosorbent assay (ELISA)

The concentrations of IL-1β and IL-18 were determined by the commercially available ELISA kits (Solarbio, Beijing, China) according to the manufacturer's protocol. Briefly, the cell culture supernatants were collected after the indicated treatment and were loaded to the ELISA plate. After 2 h of incubation at room temperature, the biotin-conjugated antibody was added to each well and incubated for 1 h. Horseradish peroxidase-labeled streptavidin and TMB substrate were added to each well in sequence and then incubated for 20 min at room temperature in the dark. Finally, stop solution was added to each well. The absorbance at 450 nm was detected using a spectrophotometric microplate reader (PerkinElmer).

qRT-PCR analysis

Total RNA in human NP tissue and degenerative NP cells were extracted by the TRIzol reagent (Invitrogen). The purity and concentration of the extracted RNA was detected by a Nanodrop 3000 (Thermo Fisher Scientific, Waltham, MA, USA). The Superscript First-Strand cDNA system kit (Thermo Fisher Scientific) was applied for the reverse transcription of extracted RNA into cDNA. Then, qRT-PCR was performed using SYBR Green Real-Time PCR Master Mix (Promega) on an ABI 7900HT Fast Real-Time PCR System (Applied Biosystems, Foster City, CA, USA). The primers for qRT-PCR were synthesized by Sangon Biotech (Shanghai, China). The primer sequences used in this study are as follows: MIR155HG (Sense 5′-GCAGGTTTTGGCTTGT TCAT-3′, Antisense 5′-AAAACGTTGCCAGACAATCC-3′), NLRP3 (Sense 5′-AAAGCCAAG AATCCACAGTGTAAC-3′, Antisense 5′-TTGCCTCGCAGGTAAAGGT-3′), GAPDH (Sense 5′-TGTGGGCATCAATGGATTTGG-3′, Antisense 5′-ACACCATGTATTCCGGGTCAAT-3′), miR-223-3p (Sense 5′-GAAGCTGTACCTAACATACCGTG-3′, Antisense 5′-GATTGGTCGTGG ACGTGTCG-3′), and U6 (Sense 5′-AGTAAGCCCTTGCTGTCAGTG-3′, Antisense 5′-CCTGGG TCTGATAATGCTGGG-3′). The specificity of all PCR products was evaluated by melting curve analysis. The expression levels of target genes were determined using the $2^{-\Delta\Delta}$Ct method, with GAPDH or U6 as endogenous controls.

Western blot analysis

The RIPA buffer containing 0.1 mmol/l phenylmethanesulfonylfluoride (Beyotime) was used to extract total proteins from human NP tissue and degenerative NP cells. The protein concentrations were determined by a BCA Protein Assay Kit (Beyotime). Equal amounts of protein lysates were separated by SDS-PAGE and then transferred to polyvinylidene difluoride membranes (Millipore, Billerica, MA, USA). After blocking with 5% skim milk at room temperature for 2 h, the membranes were incubated with the primary antibodies against NLRP3 (ab214185, 1:500), caspase-1 (ab62698, 1:500), GSDMD-N (ab215203, 1:1000) or β-actin (ab8226, 1:10000) overnight at 4°C. After washing with PBST for three times, the membranes were incubated with the secondary antibodies (1:3000) at room temperature

for 2 h. The protein bands were visualized with BeyoECL Plus kit (Beyotime) and quantified using Gel-Pro software (version 4.0). β-actin was used as an internal control.

Statistical analysis

The *in vitro* experiments were performed on three biological replicates (n=3). Data are presented as the mean ± standard deviation (SD). The GraphPad Prism 8.0 software (San Diego, CA, USA) was used for statistical analysis and figure plotting. The differences between two groups were analyzed by Student's *t*-test. The differences among ≥ three groups were analyzed using one-way ANOVA followed by Tukey's multiple comparison test. Correlation analysis was carried out using Pearson's test. A *P* value less than 0.05 was considered statistically significant.

Results

MIR155HG is highly expressed in human degenerative NP tissue

To reveal whether MIR155HG is altered during IDD, qRT-PCR was applied to detect its expression in 30 human degenerative NP tissue samples and 10 normal NP tissue samples. Compared with normal NP tissue, degenerative NP tissue displayed a marked elevation in MIR155HG expression (Fig. 1A). Further, MIR155HG expression was gradually increased with the exacerbation of disc degeneration degree (Fig. 1B). A positive correlation was also observed between MIR155HG expression and Pfirrmann score (r = 0.78, P < 0.001), as shown in Fig. 1C. These findings suggest that MIR155HG may play a role in the onset and development of IDD.

MIR155HG promotes cell pyroptosis in human degenerative NP cells

Given pyroptosis as a critical contributor to IDD, we next tested the influence of MIR155HG on NP cell pyroptosis. To this end, human degenerative NP cells were treated with PBS, LV-Mock, or LV-MIR155HG. As shown in Fig. 2A, MIR155HG expression was significantly higher in LV-MIR155HG group than that in control group, suggesting that LV-MIR155HG was successfully constructed. Importantly, MIR155HG overexpression dramatically increased the protein levels of NLRP3, caspase-1 and GSDMD-N (Fig. 2B). Consistently, MIR155HG overexpression promoted IL-1β and IL-18 secretion (Fig. 2C) and enhanced LDH release (Fig. 2D). Pyroptotic cell death was also increased upon LV-MIR155HG infection, as evidenced by Hoechst 33342/PI double fluorescence staining (Fig. 2E). Collectively, these results indicate that MIR155HG can induce the pyroptosis of human degenerative NP cells.

NLRP3 is involved in MIR155HG-induced pyroptosis of human degenerative NP cells

NLRP3 is known to play a central role in promoting cell pyroptosis. We speculated that NLRP3 may be implicated in MIR155HG-induced pyroptosis of human degenerative NP cells. To confirm this possibility, we first measured NLRP3 expression in NP tissue and cells using qRT-PCR and western blot. As expected, higher levels of NLRP3 mRNA and protein were found in human degenerative NP tissue compared with those in normal NP tissue (Fig. 3A). A significant increase in NLRP3 mRNA and protein expression was also observed when human degenerative NP cells were transfected with LV-MIR155HG (Fig. 3B). Subsequently, human degenerative NP cells were transfected with scrambled siRNA or NLRP3 siRNA. The western blot results showed an efficient knockdown of NLRP3 (Fig. 3C). Finally, human degenerative NP cells were transfected with NLRP3 siRNA and then treated with or without LV-MIR155HG. Silencing of NLRP3 by siRNA attenuated the influence of MIR155HG on caspase-1 and GSDMD-N expression (Fig. 3D), IL-1β and IL-18 secretion (Fig. 3E), and LDH release

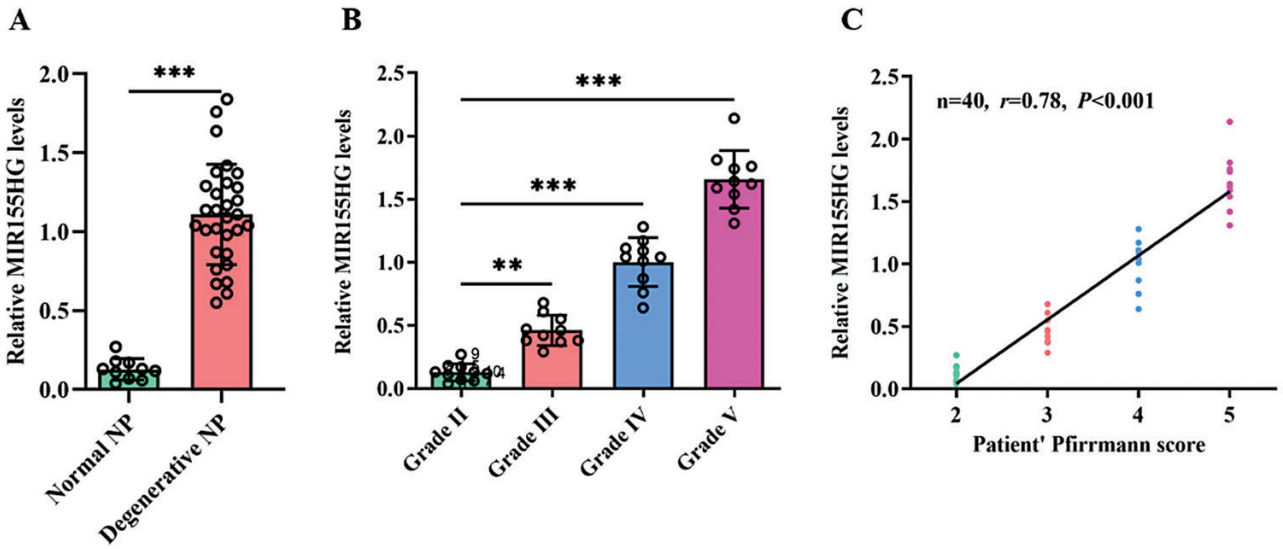

Fig. 1 MIR155HG expression in NP tissue and its correlation with Pfirrmann score. (A) The qRT-PCR was employed to detect MIR155HG expression in 10 normal human NP tissue samples (Grade II) and 30 degenerative human NP tissue samples evaluated as Grades III-V (n = 10 in each grade). (B) Comparison of MIR155HG expression in NP tissue samples with Grades II-V (n = 10 in each grade). (C) The correlation analysis between MIR155HG expression and Pfirrmann score (n = 10 in each grade). The data are expressed as mean ± SD. $^{**}P < 0.01$, $^{***}P < 0.001$.

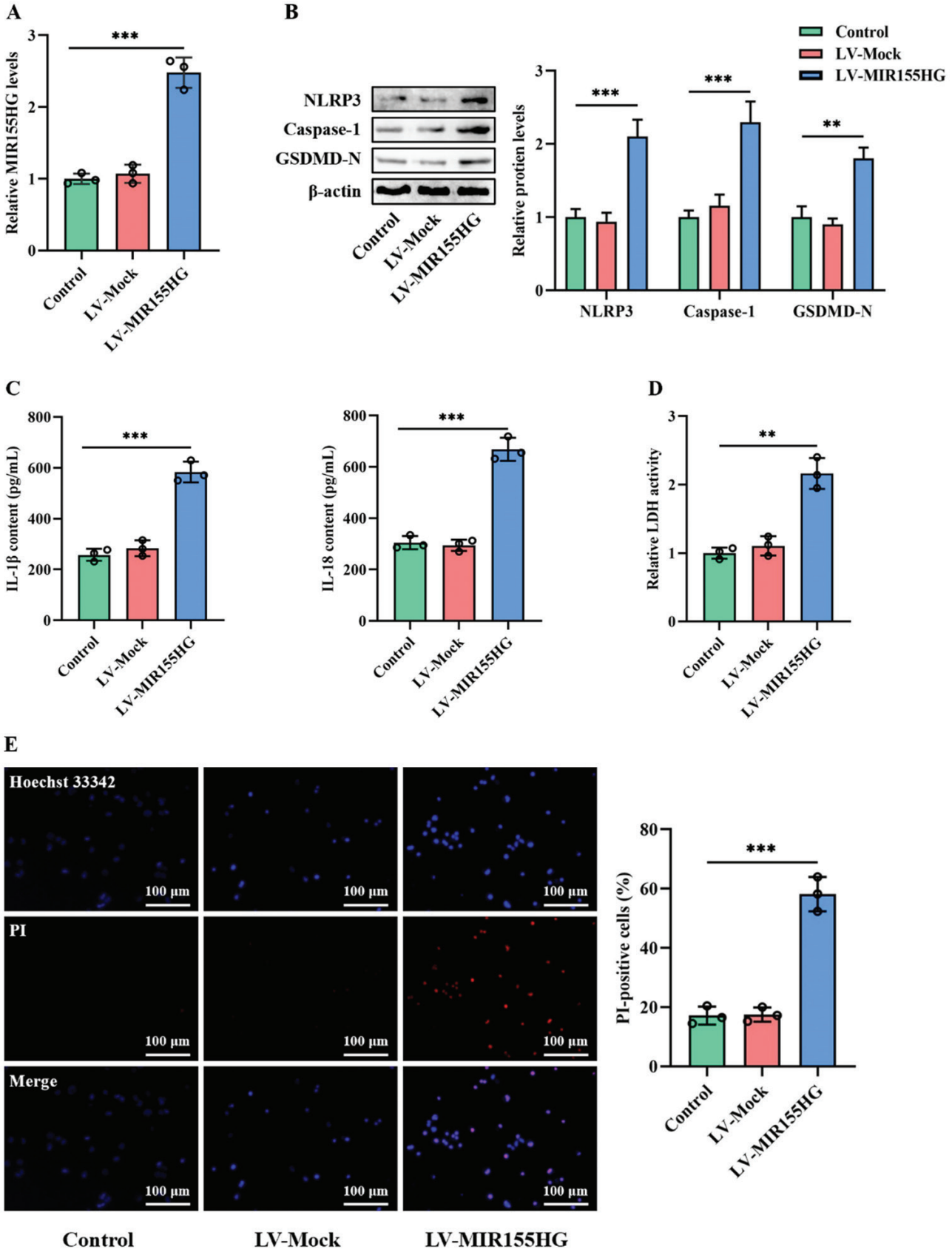

Fig. 2 Effect of MIR155HG on cell pyroptosis in human degenerative NP cells. (A–E) Human degenerative NP cells were incubated with PBS, LV-Mock, or LV-MIR155HG for 72 h. (A) MIR155HG expression was detected using qRT-PCR. (B) The western blot analysis of NLRP3, caspase-1 and GSDMD-N protein expression. (C) ELISA was applied to measure IL-1β and IL-18 levels in the cell culture supernatants. (D) Measurement of LDH activity in the cell culture supernatants using an LDH assay kit. (E) Representative images of fluorescent staining with Hoechst 33342 (blue) and PI (red) and quantitative analysis of PI positive cells. All data are presented as mean ± SD (n = 3, Grade IV). $^{**}P < 0.01$, $^{***}P < 0.001$.

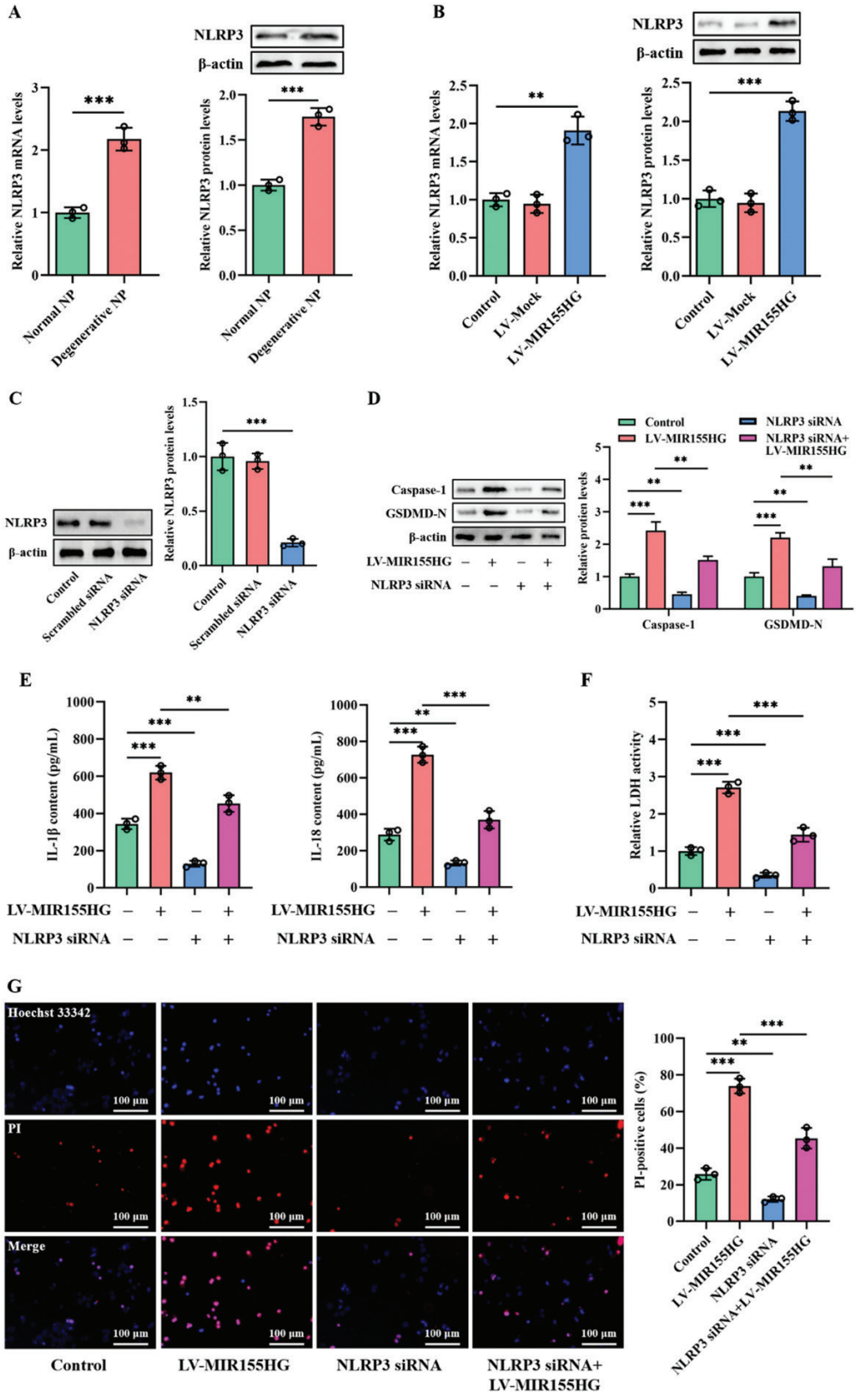

Fig. 3 Involvement of NLRP3 in MIR155HG-induced pyroptosis in human degenerative NP cells. (A) Both qRT-PCR and western blot were used to assay NLRP3 expression in 10 normal human NP tissue samples (Grade II) and 30 degenerative human NP tissue samples with Grades III-V (n = 10 in each grade). (B) Human degenerative NP cells were treated with PBS, LV-Mock, or LV-MIR155HG for 72 h, followed by detection of NLRP3 expression using qRT-PCR and western blot (n = 3, Grade IV). (C) Human degenerative NP cells were transfected with scrambled siRNA or NLRP3 siRNA for 48 h. Cell lysates were immunoblotted with the antibodies against NLRP3 or β-actin (n = 3, Grade IV). (D–G) Human degenerative NP cells were transfected with NLRP3 siRNA for 48 h and then transduced with or without LV-MIR155HG for an additional 72 h (n = 3, Grade IV). (D) The western blot analysis of caspase-1 and GSDMD-N protein expression. (E) Detection of IL-1β and IL-18 levels in the cell culture supernatants using ELISA. (F) The LDH assay kit was used to measure LDH activity in the cell culture supernatants. (G) Representative images of fluorescent staining with Hoechst 33342 (blue) and PI (red). PI-positive cells were quantified. Data shown are mean ± SD. $^{*}P < 0.05$, $^{**}P < 0.01$, $^{***}P < 0.001$.

(Fig. 3F). Also, the promotive effect of MIR155HG on pyroptotic cell death was reversed by NLRP3 knockdown (Fig. 3G). These observations suggest that NLRP3 is necessary for MIR155HG-induced pyroptosis of human degenerative NP cells.

Identification of NLRP3 as a direct target of miR-223-3p

By using the TargetScan and miRDB databases, we found that there was a binding site present between miR-223-3p and NLRP3 3′UTR (Fig. 4A). Further, the RNAhybrid software revealed a lower free energy score for the interaction of miR-223-3p with NLRP3 3′UTR (–13.0 kcal/mol), suggesting that miR-223-3p is able to bind stably to NLRP3 3′UTR (Fig. 4B). To validate the predicted results by the bioinformatics, we constructed NLRP3-WT and NLRP3-Mut plasmids (Fig. 4A). These plasmids were co-transfected into 293T cells with miR-223-3p mimic or mimic control, followed by detection of luciferase activity. Transfection with miR-223-3p mimic dramatically decreased the luciferase activity of NLRP3-WT but not NLRP3-Mut (Fig. 4C). Thereafter, human degenerative NP cells were transfected with miR-223-3p mimic, mimic control, miR-223-3p inhibitor or inhibitor control. The qRT-PCR results demonstrated that miR-223-3p mimic markedly increased, whereas its inhibitor decreased, miR-223-3p levels, thereby suggesting a high transfection efficacy (Fig. 4D). Meanwhile, miR-223-3p overexpression attenuated the mRNA and protein levels of NLRP3, whereas miR-223-3p inhibition had an opposite effect on NLRP3 expression (Fig. 4E). Thus, these findings identify NLRP3 as a direct target of miR-223-3p, confirming the previous reports [31, 32].

MIR155HG functions as a ceRNA of miR-223-3p

LncRNAs can interact with miRNAs to increase the expression levels of mRNAs, an action mode called ceRNA [33]. By using the Starbase database, we found that MIR155HG shared a common miR-223-3p binding site with NLRP3 (Fig. 5A). The constructed MIR155HG-WT and MIR155HG plasmids were co-transfected into 293T cells with miR-223-3p mimic or mimic control. Our results showed that miR-223-3p overexpression reduced the luciferase activity of MIR155HG-WT but had no impact on the luciferase activity of MIR155HG-Mut (Fig. 5B). To further confirm the interaction between miR-223-3p and MIR155HG, a bio-miR-223-3p pulldown assay was employed to determine whether miR-223-3p could pull down MIR155HG in human degenerative NP cells. As illustrated in Fig. 5C, MIR155HG was pull down by bio-miR-223-3p-WT but not bio-miR-223-3p-Mut, suggesting that miR-223-3p can bind directly

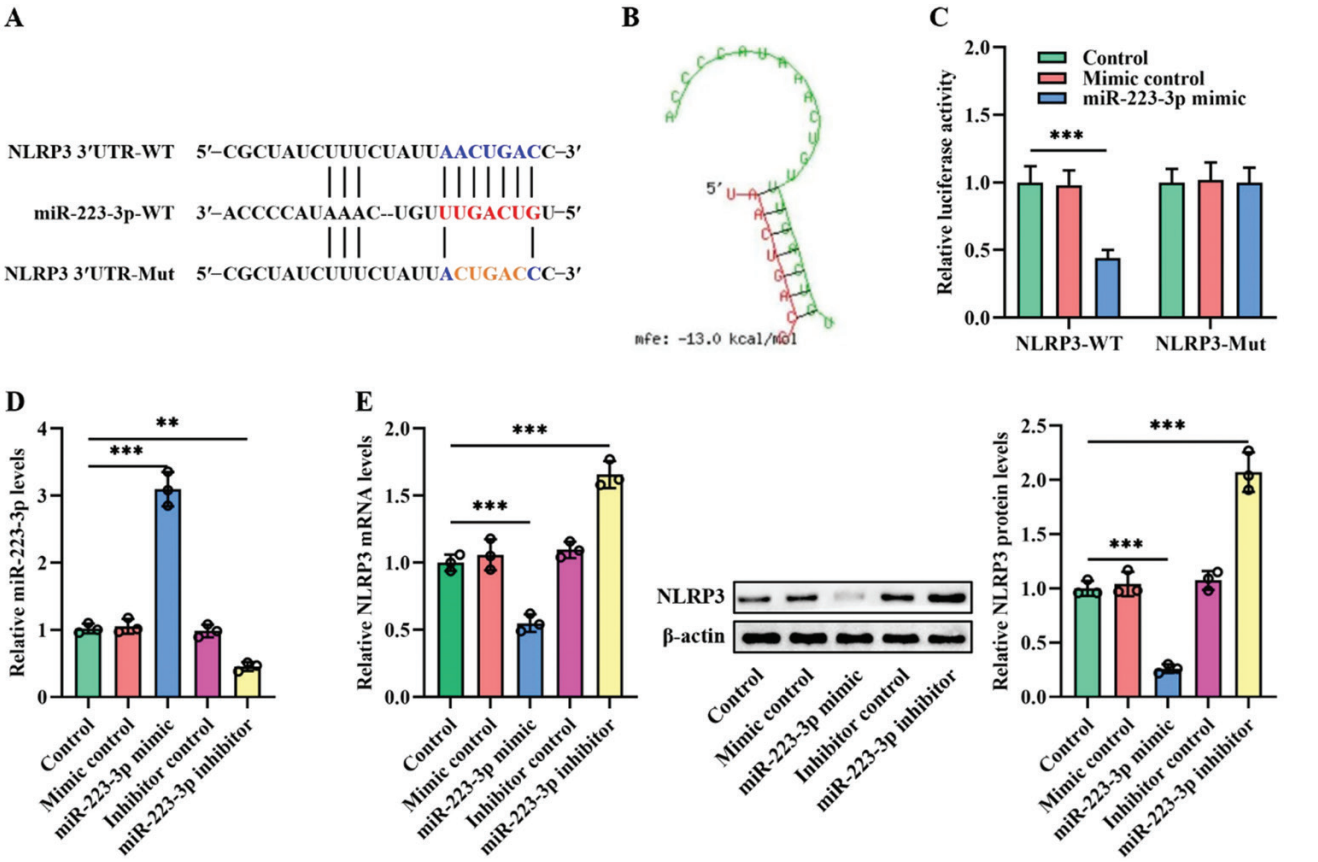

Fig. 4 NLRP3 is identified as a direct target of miR-223-3p. (A) Schematic illustration of the binding site between miR-223-3p and NLRP3 3′UTR and corresponding mutation. (B) Free energy score predicted by the RNAhybrid database. (C) The NLRP3-WT and NLRP3-Mut plasmids were co-transfected into 293T cells with miR-223-3p mimic or mimic control. After 48 h of transfection, the luciferase activity were detected ($n = 3$). (D and E) Following transfection of human degenerative NP cells with miR-223-3p mimic/inhibitor or their negative controls for 48 h, the expression of miR-223-3p and NLRP3 was evaluated by qRT-PCR and/or western blot ($n = 3$, Grade IV). Data represent the mean ± SD. $^{**}P < 0.01$, $^{***}P < 0.001$.

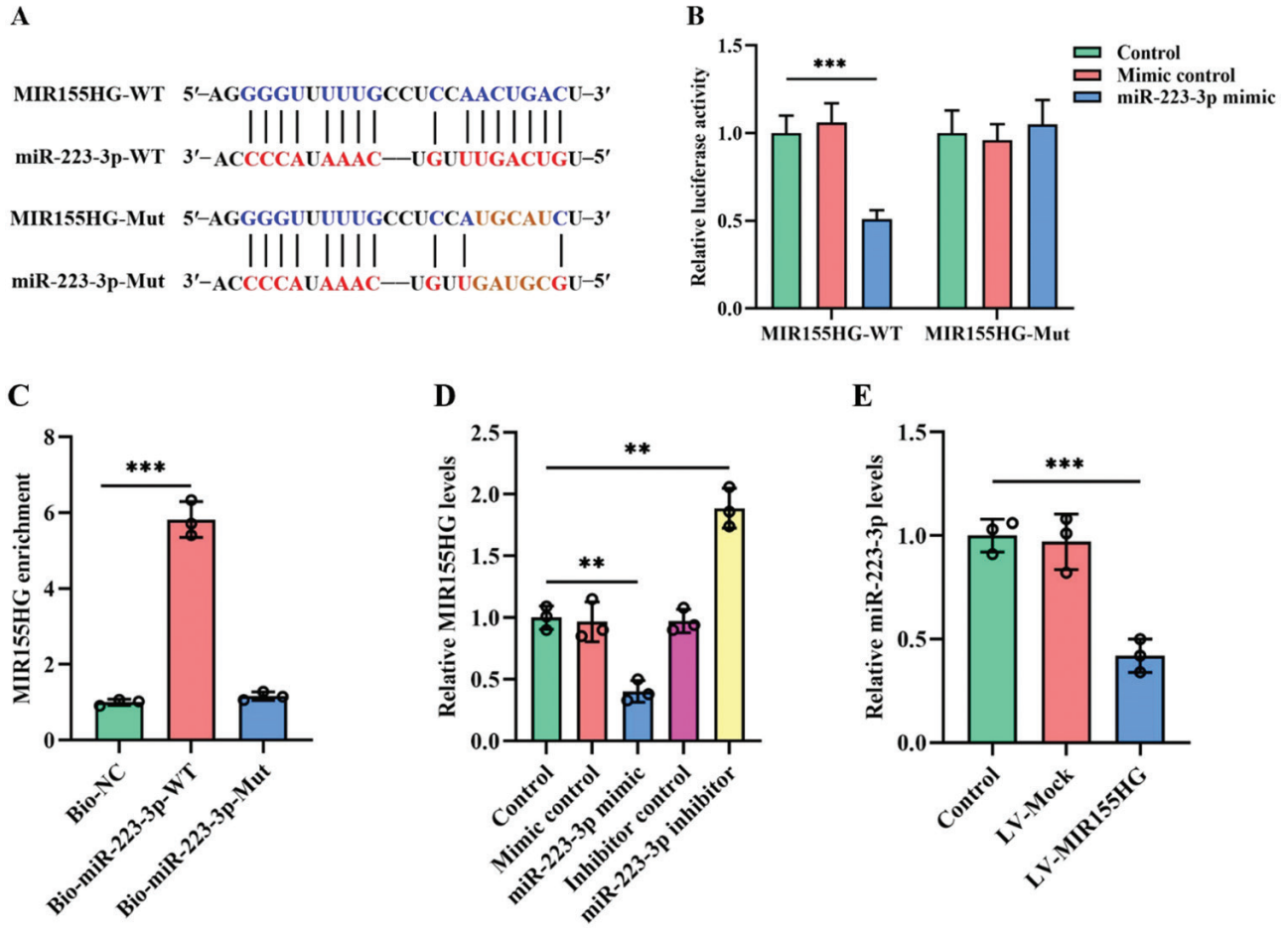

Fig. 5 Identification MIR155HG as a ceRNA of miR-223-3p. (A) Schematic drawing of the binding site between miR-223-3p and MIR155HG and corresponding mutation. (B) The 293T cells were co-transfected with MIR155HG-WT/Mut plasmids and miR-223-3p mimic/mimic control for 48 h, followed by detection of luciferase activity (n=3). (C) Human degenerative NP cells were treated with bio-miR-223-3p-WT, bio-miR-223-3p-Mut, or bio-miR-NC for 48 h, and pulldown assay was performed (n = 3, Grade IV). (D) Following transfection of human degenerative NP cells with miR-223-3p mimic/inhibitor or their negative controls for 48 h, qRT-PCR was employed to analyze MIR155HG expression (n = 3, Grade IV). (E) Human degenerative NP cells were incubated with PBS, LV-Mock, or LV-MIR155HG for 72 h, followed by measurement of miR-223-3p expression using qRT-PCR (n = 3, Grade IV). The data are represented as mean ± SD. $^{**}P < 0.01$, $^{***}P < 0.001$.

to MIR155HG. Subsequently, we detected MIR155HG expression in human degenerative NP cells transfected with miR-223-3p mimic/inhibitor. Overexpression of miR-223-3p diminished MIR155HG levels, whereas its inhibition enhanced MIR155HG levels (Fig. 5D). The expression of miR-223-3p and NLRP3 was also measured in human degenerative NP cells transduced with LV-MIR155HG. In comparison with control group, LV-MIR155HG group displayed a significant decrease in miR-223-3p levels (Fig. 5E) as well as a significant increase in NLRP3 mRNA and protein expression (Fig. 3B). To summarize, these results indicate the existence of specific cross-talk between MIR155HG and NLRP3 through competition for miR-223-3p binding.

miR-223-3p is required for induction of NLRP3 expression and cell pyroptosis by MIR155HG

Having identified a ceRNA network among MIR155HG, miR-223-3p and NLRP3, we next explored whether miR-223-3p was involved in the promotive effect of MIR155HG on NLRP3 expression and cell pyroptosis in human degenerative NP cells. When compared with normal NP tissue samples, human degenerated NP tissue samples exhibited a significant decrease in miR-223-3p levels (Fig. 6A). Afterward, human degenerative NP cells were transfected with miR-223-3p mimic prior to LV-MIR155HG treatment. As anticipated, the increase in NLRP3 mRNA and protein expression by LV-MIR155HG was suppressed by miR-223-3p mimic (Fig. 6B). In addition, pretreatment with miR-223-3p mimic significantly reversed LV-MIR155HG-induced enhancement of caspase-1 and GSDMD-N expression (Fig. 6C), IL-1β and IL-18 secretion (Fig. 6D), LDH release (Fig. 6E), and pyroptotic cell death (Fig. 6F). These data suggest that MIR155HG increases NLRP3 levels and stimulates cell pyroptosis by down-regulating miR-223-3p expression in human degenerative NP cells.

Discussion

IDD constitutes the pathological basis of degenerative disc disease. In the recent years, its incidence is gradually increased. MIR155HG is a lncRNA with a pro-inflammatory effect [34]. However, very little is known about its association with IDD. In the present study, we observed a marked elevation of MIR155HG expression in human degenerative NP tissue compared with normal NP tissue. Moreover, its expression

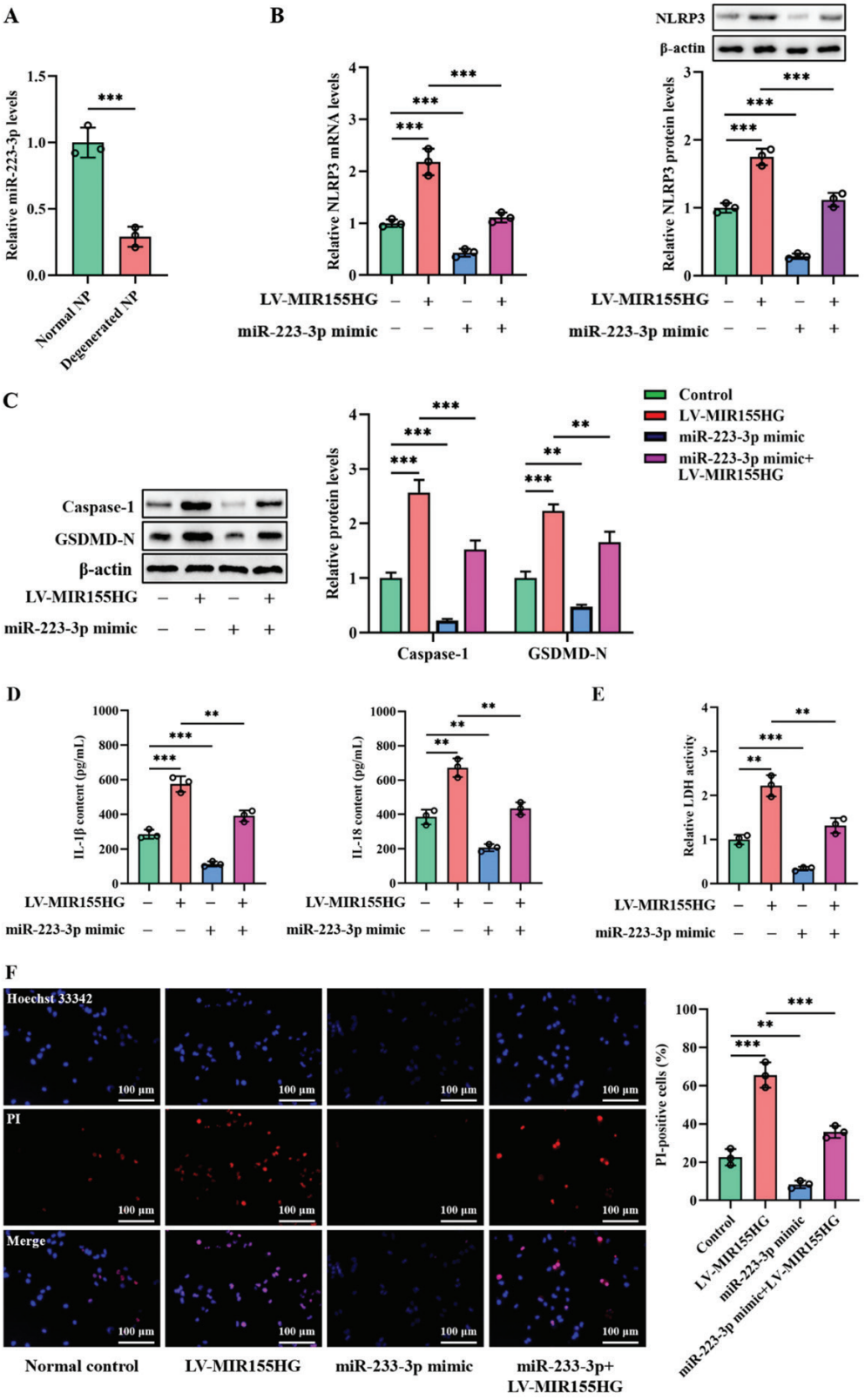

Fig. 6 MIR155HG increases NLRP3 expression and induces cell pyroptosis by sponging miR-223-3p in human degenerative NP cells. (A) Detection of miR-223-3p expression in 10 normal human NP tissue samples (Grade II) and 30 degenerative human NP tissue samples with Grades III-V (n = 10 in each grade) using qRT-PCR. (B–F) Human degenerative NP cells were transfected with miR-223-3p mimic for 48 h, followed by treatment with or without LV-MIR155HG for an additional 72 h (n = 3, Grade IV). (B) The qRT-PCR and western blot analyses of NLRP3 expression. (C) Western blot was used to determine the protein levels of caspase-1 and GSDMD-N. (D) Detection of IL-1β and IL-18 levels in the cell culture supernatants using ELISA. (E) Detection of LDH activity in the cell culture supernatants using the LDH assay kit. (F) Representative images of fluorescent staining with Hoechst 33342 (blue) and PI (red) and quantitative analysis of PI positive cells. The data are shown as mean ± SD. $^{**}P < 0.01$, $^{***}P < 0.001$, $^{\#}P < 0.05$.

levels increased with the severity of disease and showed a positive correlation with Pfirrmann score. These results first reveal a close link of MIR155HG to IDD. MIR155HG may be a potential biomarker to reflect the severity of IDD.

Inflammation and intervertebral disk cell death are two major features of IDD [35–38]. Pyroptosis, a newly discovered programmed cell death, is different from apoptosis and necrosis [39, 40]. After activation, the N-terminal pyrin segment of NLRP3 interacts with ASC to recruit pro-caspase-1. Subsequently, pro-caspase-1 undergoes autoproteolytic cleavage to become active caspase-1. As a cysteine-dependent protease, active caspase-1 cleaves GSDMD, pro-IL-1β and pro-IL-18 into GSDMD-N, IL-1β, and IL-18, respectively. GSDMD-N promotes membrane pore formation and causes cell rupture, thereby leading to the release of IL-1β and IL-18 [41]. Increased NP cell pyroptosis is observed in degenerative NP tissue [42]. Promoting NP cell pyroptosis was shown to accelerate IDD in animal models [43, 44]. Both IL-1β and IL-18 not only promote the infiltration of immune cells and induce an inflammatory cascade but also contribute to extracellular matrix degradation [45, 46]. All of these processes impair the health of intervertebral disk, thereby leading to the occurrence and development of IDD. It has been reported that MIR155HG can enhance the production of pro-inflammatory cytokines in multiple cell types [10–12]. Similarly, we found that lentivirus-mediated overexpression of MIR155HG stimulated human degenerative NP cell pyroptosis and promoted the release of IL-1β and IL-18. Thus, MIR155HG may play a detrimental role in the development of IDD. Degenerative NP cells are more sensitive to pyroptosis than non-degenerative NP cells. If non-degenerative NP cells are used to investigate pyroptosis, lipopolysaccharide is usually applied to establish the cell pyroptosis model [5]. Moreover, to the best of our knowledge, the vast majority of studies selected degenerative NP cells as a cell model to expolre the influence on pyroptosis [28, 47]. In line with these studies, we performed MIR155HG overexpression experiments in degenerative NP cells rather than non-degenerative NP cells.

The hypothesis of ceRNA was first proposed by Salmena *et al.* in 2011 [48]. As an important mode of gene expression modulation, the ceRNA network highlights that the specific RNAs with common miRNA binding sites compete for post-transcriptional control [49]. A recent study showed that MIR155HG acts as a ceRNA to promote glioblastoma growth and progression [50]. miR-223-3p is a highly conserved miRNA in vertebrates. Administration of sinomenine, a major bioactive component of *Sinomenium acutum*, attenuates serum TNF-α, IL-1β, IL-6, and IL-18 levels and alleviates articular cartilage degradation by up-regulating miR-223-3p expression in a mouse model of osteoarthritis [51]. NLRP3 is currently the most studied inflammasome. Recently, He *et al.* reported that propionibacterium acnes infection promotes cell pyroptosis in human degenerative NP cells and aggravates IDD in rabbits by activating the thioredoxin binding protein/NLRP3 pathway [43]. Treatment with notoginsenoside Rg1, the major effective component of Panax notoginseng, inhibits cell pyroptosis and inflammatory response in rat NP cells challenged with TNF-α by down-regulating NLRP3 expression [52]. In addition, miR-223-3p was shown to attenuate cell pyroptosis by silencing of NLRP3 in multiple cell types [20–22]. In this study, we identified a ceRNA regulatory network among MIR155HG, miR-223-3p, and NLRP3. Further, the promotive effect of MIR155HG on human degenerative NP cell pyroptosis was reversed by pretreatment with miR-223-3p mimic or NLRP3 siRNA, suggesting the involvement of the miR-223-3p/NLRP3 axis in MIR155HG-induced pyroptosis of human degenerative NP cells.

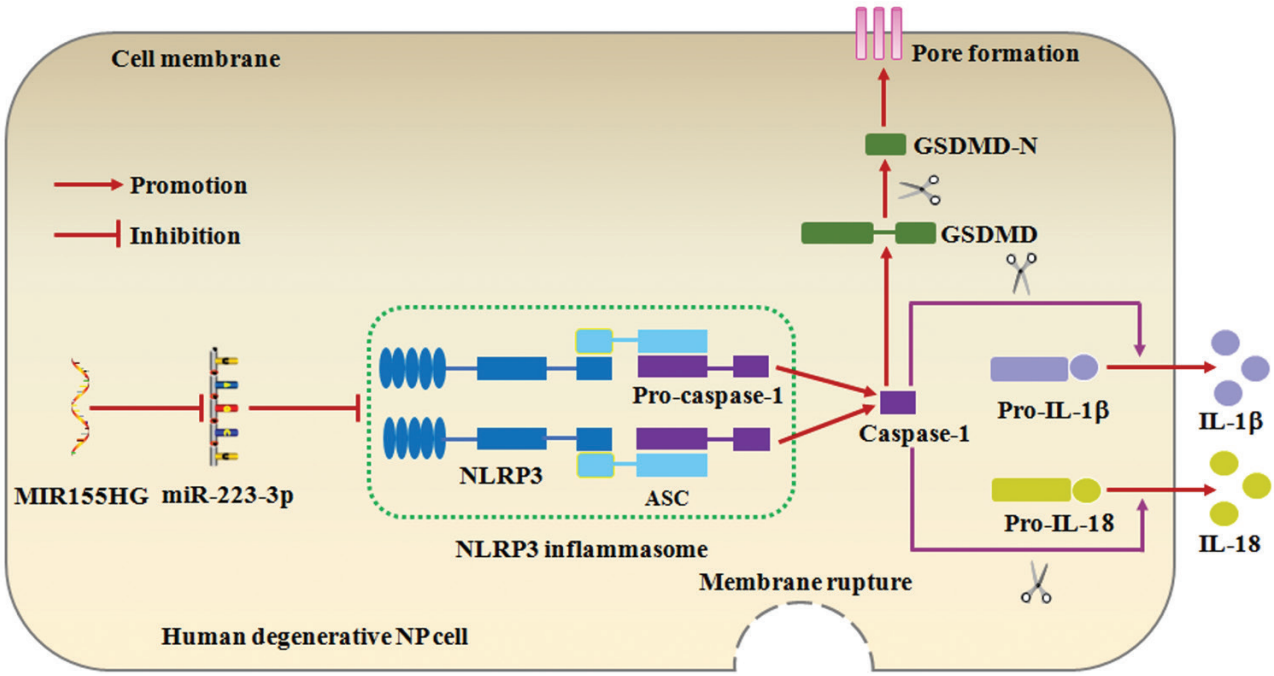

Fig. 7 A schematic showing MIR155HG-induced pyroptosis of human degenerative NP cells. MIR155HG up-regulates NLRP3 expression by acting as a ceRNA for miR-223-3p. This leads to activation of the NLRP3 inflammasome, formation of membrane pores and release of IL-1β and IL-18 from human degenerative NP cells.

Despite we clearly demonstrate that MIR155HG stimulates human degenerative NP cell pyroptosis through the miR-223-3p/NLRP3 signaling pathway, there are several limitations in this study. Firstly, we do not perform animal experiments to observe the *in vivo* effects of MIR155HG on miR-223-3p and NLRP3 expression, NP cell pyroptosis, and IDD. Secondly, given that lncRNAs can regulate gene expression through multiple mechanisms of action [53], it is possible that MIR155HG affects NP cell pyroptosis through other pathways besides the ceRNA network. Thirdly, IDD is a complex and multifactorial disease involved in numerous pathophysiological processes, including imbalance of extracellular matrix anabolism and catabolism, autoimmune response and oxidative stress [54–56]. However, we do not explore the impact of MIR155HG on these biological behaviors. Finally, it remains to be determined whether MIR155HG plays a role in regulating annulus fibrosis cell pyroptosis.

Conclusion

Taken together, we have demonstrated that MIR155HG plays an important promotive role in human degenerative NP cell pyroptosis. Mechanistically, MIR155HG functions as a ceRNA of miR-223-3p to increase NLRP3 expression (Fig. 7). With continued efforts, blockade of MIR155HG could become a novel and promising strategy for the prevention and treatment of degenerative disc disease.

Acknowledgement

We thank Xiao-Hua Yu and Jiao-Jiao Chen for their help and advices in the cellular experiments.

Funding

This study was supported by research funds from the Health Commission of Hunan Province (C2019112) and Natural Science Foundation in Hunan Province (2021JJ50099) in China.

Conflict of interest

The authors declare they do not have anything to disclose regarding conflicts of interest with respect to this manuscript.

Author contributions

W.Y. and J.Z. designed the research and wrote the paper. W.Y., X.-D.H. and T.Z. performed the experiments. Y.-B.Z. collected tissue samples. Y.-C.Z. analyzed the data.

Data availability

The data are available from the corresponding author on reasonable request.

References

1. Global Burden of Disease Study 2013 Collaborators. Global, regional, and national incidence, prevalence, and years lived with disability for 301 acute and chronic diseases and injuries in 188 countries, 1990-2013: a systematic analysis for the Global Burden of Disease Study 2013. *Lancet*. 2015, 386(9995), 743–800.
2. Zhang F, Zhao X, Shen H, Zhang C. Molecular mechanisms of cell death in intervertebral disc degeneration (Review). *Int J Mol Med* 2016, 37, 1439–48.
3. Lyu FJ, Cui H, Pan H, et al. Painful intervertebral disc degeneration and inflammation: from laboratory evidence to clinical interventions. *Bone Res* 2021, 9, 7.
4. Wang Y, Peng J, Xie X, Zhang Z, Li M, Yang M. Gasdermin E-mediated programmed cell death: an unpaved path to tumor suppression. *J Cancer* 2021, 12, 5241–8.
5. Liao Z, Li S, Liu R, et al. Autophagic degradation of Gasdermin D protects against nucleus Pulposus cell Pyroptosis and retards Intervertebral disc degeneration in vivo. *Oxid Med Cell Longev* 2021, 2021, 5584447.
6. Zhou Y, Chen Z, Yang X, et al. Morin attenuates pyroptosis of nucleus pulposus cells and ameliorates intervertebral disc degeneration via inhibition of the TXNIP/NLRP3/Caspase-1/IL-1β signaling pathway. *Biochem Biophys Res Commun* 2021, 559, 106–12.
7. Zhang Z, Huo Y, Zhou Z, Zhang P, Hu J. Role of lncRNA PART1 in intervertebral disc degeneration and associated underlying mechanism. *Exp Ther Med* 2021, 21, 131.
8. Cui S, Liu Z, Tang B, Wang Z, Li B. LncRNA MAGI2-AS3 is downregulated in intervertebral disc degeneration and participates in the regulation of FasL expression in nucleus pulposus cells. *BMC Musculoskelet Disord* 2020, 21, 149.
9. Tang N, Dong Y, Xiao T, Zhao H. LncRNA TUG1 promotes the intervertebral disc degeneration and nucleus pulposus cell apoptosis though modulating miR-26a/HMGB1 axis and regulating NF-κB activation. *Am J Transl Res* 2020, 12, 5449–64.
10. Li N, Liu Y, Cai J. LncRNA MIR155HG regulates M1/M2 macrophage polarization in chronic obstructive pulmonary disease. *Biomed Pharmacother* 2019, 117, 109015.
11. Song J, Wang Q, Zong L. LncRNA MIR155HG contributes to smoke-related chronic obstructive pulmonary disease by targeting miR-128-5p/BRD4 axis. *Biosci Rep*. 2020, 40, BSR20192567.
12. Zhang C, Li J, Li H, et al. lncRNA MIR155HG accelerates the progression of sepsis via upregulating MEF2A by sponging miR-194-5p. *DNA Cell Biol* 2021, 40, 811–20.
13. Wang C, Wang WJ, Yan YG, et al. MicroRNAs: new players in intervertebral disc degeneration. *Clin Chim Acta* 2015, 450, 333–41.
14. Wang WJ, Yang W, Ouyang ZH, et al. MiR-21 promotes ECM degradation through inhibiting autophagy via the PTEN/akt/mTOR signaling pathway in human degenerated NP cells. *Biomed Pharmacother* 2018, 99, 725–34.
15. Wang J, Liu X, Sun B, Du W, Zheng Y, Sun Y. Upregulated miR-154 promotes ECM degradation in intervertebral disc degeneration. *J Cell Biochem*. 2019, 120, 11900–7.
16. Hasvik E, Schjølberg T, Jacobsen DP, et al. Up-regulation of circulating microRNA-17 is associated with lumbar radicular pain following disc herniation. *Arthritis Res Ther* 2019, 21, 186.
17. Rodríguez AE, Hernández JÁ, Benito R, et al. Molecular characterization of chronic lymphocytic leukemia patients with a high number of losses in 13q14. *PLoS One* 2012, 7, e48485.
18. Moen A, Jacobsen D, Phuyal S, et al. MicroRNA-223 demonstrated experimentally in exosome-like vesicles is associated with decreased risk of persistent pain after lumbar disc herniation. *J Transl Med* 2017, 15, 89.
19. Wang H, Hao P, Zhang H, Xu C, Zhao J. MicroRNA-223 inhibits lipopolysaccharide-induced inflammatory response by directly targeting Irak1 in the nucleus pulposus cells of intervertebral disc. *IUBMB Life* 2018, 70, 479–90.
20. Long FQ, Kou CX, Li K, Wu J, Wang QQ. MiR-223-3p inhibits rTp17-induced inflammasome activation and pyroptosis by targeting NLRP3. *J Cell Mol Med* 2020, 24, 14405–14.
21. Ren N, Jiang T, Wang C, et al. LncRNA ADAMTS9-AS2 inhibits gastric cancer (GC) development and sensitizes chemoresistant GC

cells to cisplatin by regulating miR-223-3p/NLRP3 axis. *Aging (Albany NY)* 2020, 12, 11025–41.
22. Tian J, Zhou D, Xiang L, et al. MiR-223-3p inhibits inflammation and pyroptosis in monosodium urate-induced rats and fibroblast-like synoviocytes by targeting NLRP3. *Clin Exp Immunol* 2021, 204, 396–410.
23. Tay Y, Rinn J, Pandolfi PP. The multilayered complexity of ceRNA crosstalk and competition. *Nature* 2014, 505, 344–52.
24. Qi X, Zhang DH, Wu N, Xiao JH, Wang X, Ma W. ceRNA in cancer: possible functions and clinical implications. *J Med Genet* 2015, 52, 710–8.
25. Zhang YH, Song J, Shen L, Shao J. Systematic identification of lncRNAs and circRNAs-associated ceRNA networks in human lumbar disc degeneration. *Biotech Histochem* 2019, 94, 606–16.
26. Fan X, Chen G, Ma F, et al. An lncRNA-miRNA-mRNA-ceRNA network regulates intervertebral disc degeneration: a bioinformatics study based on the dataset analysis. *Gen Physiol Biophys* 2021, 40, 317–27.
27. Yang Y, Zhong Z, Zhao Y, Ren K, Li N. LincRNA-SLC20A1 (SLC20A1) promotes extracellular matrix degradation in nucleus pulposus cells in human intervertebral disc degeneration by targeting the miR-31-5p/MMP3 axis. *Int J Clin Exp Pathol* 2019, 12, 3632–43.
28. Bai Z, Liu W, He D, et al. Protective effects of autophagy and NFE2L2 on reactive oxygen species-induced pyroptosis of human nucleus pulposus cells. *Aging (Albany NY)* 2020, 12, 7534–48.
29. Jiang Y, Liu H, Yu H, et al. Circular RNA Calm4 regulates hypoxia-induced pulmonary arterial smooth muscle cells pyroptosis via the Circ-Calm4/miR-124-3p/PDCD6 axis. *Arterioscler Thromb Vasc Biol* 2021, 41, 1675–93.
30. Yu XH, Deng WY, Chen JJ, et al. LncRNA kcnq1ot1 promotes lipid accumulation and accelerates atherosclerosis via functioning as a ceRNA through the miR-452-3p/HDAC3/ABCA1 axis. *Cell Death Dis* 2020, 11, 1043.
31. Jimenez Calvente C, Del Pilar H, Tameda M, Johnson CD, Feldstein AE. MicroRNA 223 3p negatively regulates the NLRP3 inflammasome in acute and chronic liver injury. *Mol Ther* 2020, 28, 653–63.
32. Wang X, Chi J, Dong B, et al. MiR-223-3p and miR-22-3p inhibit monosodium urate-induced gouty inflammation by targeting NLRP3. *Int J Rheum Dis* 2021, 24, 599–607.
33. Yamamura S, Imai-Sumida M, Tanaka Y, Dahiya R. Interaction and cross-talk between non-coding RNAs. *Cell Mol Life Sci* 2018, 75, 467–84.
34. Elton TS, Selemon H, Elton SM, Parinandi NL. Regulation of the MIR155 host gene in physiological and pathological processes. *Gene* 2013, 532, 1–12.
35. Cosamalón-Gan I, Cosamalón-Gan T, Mattos-Piaggio G, Villar-Suárez V, García-Cosamalón J, Vega-Álvarez JA. Inflammation in the intervertebral disc herniation. *Neurocirugia (Astur: Engl Ed)* 2021, 32, 21–35.
36. Cunha C, Silva AJ, Pereira P, Vaz R, Gonçalves RM, Barbosa MA. The inflammatory response in the regression of lumbar disc herniation. *Arthritis Res Ther* 2018, 20, 251.
37. Stich S, Jagielski M, Fleischmann A, et al. Degeneration of lumbar intervertebral discs: characterization of Anulus Fibrosus tissue and cells of different degeneration grades. *Int J Mol Sci*. 2020, 21, 2165.
38. Ding F, Shao ZW, Xiong LM. Cell death in intervertebral disc degeneration. *Apoptosis* 2013, 18, 777–85.
39. Shi J, Gao W, Shao F. Pyroptosis: gasdermin-mediated programmed necrotic cell death. *Trends Biochem Sci* 2017, 42, 245–54.
40. Frank D, Vince JE. Pyroptosis versus necroptosis: similarities, differences, and crosstalk. *Cell Death Differ* 2019, 26, 99–114.
41. Bergsbaken T, Fink SL, den Hartigh AB, Loomis WP, Cookson BT. Coordinated host responses during pyroptosis: caspase-1-dependent lysosome exocytosis and inflammatory cytokine maturation. *J Immunol* 2011, 187, 2748–54.
42. Zhang J, Zhang J, Zhang Y, et al. Mesenchymal stem cells-derived exosomes ameliorate intervertebral disc degeneration through inhibiting pyroptosis. *J Cell Mol Med* 2020, 24, 11742–54.
43. He D, Zhou M, Bai Z, Wen Y, Shen J, Hu Z. Propionibacterium acnes induces intervertebral disc degeneration by promoting nucleus pulposus cell pyroptosis via NLRP3-dependent pathway. *Biochem Biophys Res Commun* 2020, 526, 772–9.
44. Tang G, Han X, Lin Z, et al. Propionibacterium acnes accelerates intervertebral disc degeneration by inducing pyroptosis of nucleus pulposus cells via the ROS-NLRP3 pathway. *Oxid Med Cell Longev* 2021, 2021, 4657014.
45. Yang W, Yu XH, Wang C, et al. Interleukin-1β in intervertebral disk degeneration. *Clin Chim Acta* 2015, 450, 262–72.
46. Ye S, Ju B, Wang H, Lee KB. Bone morphogenetic protein-2 provokes interleukin-18-induced human intervertebral disc degeneration. *Bone Joint Res* 2016, 5, 412–8.
47. Zhao K, An R, Xiang Q, et al. Acid-sensing ion channels regulate nucleus pulposus cell inflammation and pyroptosis via the NLRP3 inflammasome in intervertebral disc degeneration. *Cell Prolif* 2021, 54, e12941.
48. Salmena L, Poliseno L, Tay Y, Kats L, Pandolfi PP. A ceRNA hypothesis: the Rosetta Stone of a hidden RNA language? *Cell* 2011, 146, 353–8.
49. Thomson DW, Dinger ME. Endogenous microRNA sponges: evidence and controversy. *Nat Rev Genet* 2016, 17, 272–83.
50. Wu W, Yu T, Wu Y, Tian W, Zhang J, Wang Y. The miR155HG/miR-185/ANXA2 loop contributes to glioblastoma growth and progression. *J Exp Clin Cancer Res* 2019, 38, 133.
51. Dong HC, Li PN, Chen CJ, et al. Sinomenine attenuates cartilage degeneration by regulating miR-223-3p/NLRP3 inflammasome signaling. *Inflammation* 2019, 42, 1265–75.
52. Tang K, Su W, Huang C, Wu Y, Wu X, Lu H. Notoginsenoside R1 suppresses inflammatory response and the pyroptosis of nucleus pulposus cells via inactivating NF-κB/NLRP3 pathways. *Int Immunopharmacol* 2021, 101, 107866.
53. Ulitsky I, Bartel DP. lincRNAs: genomics, evolution, and mechanisms. *Cell* 2013, 154, 26–46.
54. Feng H, Danfelter M, Strömqvist B, Heinegård D. Extracellular matrix in disc degeneration. *J Bone Joint Surg Am* 2006, 88 (Suppl 2), 25–9.
55. Di Martino A, Merlini L, Faldini C. Autoimmunity in intervertebral disc herniation: from bench to bedside. *Expert Opin Ther Targets* 2013, 17, 1461–70.
56. Feng C, Yang M, Lan M, et al. ROS: crucial intermediators in the pathogenesis of intervertebral disc degeneration. *Oxid Med Cell Longev* 2017, 2017, 5601593.